Proceedings of the 17th World Congress
The International Federation of Automatic Control
Seoul, Korea, July 6-11, 2008

Macroscopic drive chain efficiency modeling using state machines

Omar Al Assad*, Emmanuel Godoy and Vincent Croulard*****

** Vascular Positionner Engineering department at General Electric Healthcare*
Buc, France (Tel: +33 1 30 70 95 12, e-mail: Omar.AlAssad@ge.com).
*** Professor at SUPELEC*
Gif-sur-Yvette, France (e-mail: Emmanuel.Godoy@supelec.fr).
**** Senior Engineer (General Electric Healthcare)*
Buc, France (e-mail: Vincent.Croulard@med.ge.com).

Abstract: In this paper, we propose a new approach to model irreversibility in robotic drive chains. Actually, some types of gears such as worm gears have an efficiency which varies according to the power flow direction. The irreversibility appears when the efficiency tends to zero in one direction only, usually, from the load to the motor. The proposed methodology consists of using a state machine to describe the functional state of drive chain. For each state, an efficiency coefficient that characterizes the power loss is defined. This technique gives conclusive results during experimental validation and allows reproducing a reliable robot simulator. This simulator is set up for the purpose of position control of a medical positioning robot.

1. INTRODUCTION

Modern control theories in robotics are more and more turned towards model-based controllers such as computed torque controllers, adaptive controllers or feedforward dynamic compensators. Therefore, dynamic modeling has become an inevitable step during controller design. Besides, accurate dynamic modeling is a key point for simulations during the mechanism design process.

In the literature, the problem of robot dynamic modeling is treated in two steps. The first one concerns the mechanical behavior of the robot external structure considered often as a rigid structure. Many researchers have treated this problem and different techniques have been introduced in order to solve this issue. The two best-known methods in this matter are the Newton-Euler formulation and the Lagrange formulation (Khalil, 2002).

The second step concerns the drive chain modeling, which includes motors, gears and power loss modeling. Despite the advances made in the field of mechanical modeling, some issues are still without a convenient solution. We can mention, for instance, the phenomenon of irreversibility that characterizes certain types of mechanical transmissions such as worm gears (Henriot, 1991). This characteristic is often required for security reasons like locking the joint in case of motor failure or unexpected current cut-off. The purpose of this paper is to present a new modeling approach based on a state machine in order to simulate irreversible transmissions.

This paper is organized as follows. In section 2, we give a brief overview of the LCA vascular robot, which is used as an application for this study. Section 3 presents details about the modeling approach used for the robot structure and drive chain. Section 4 presents the irreversibility modeling issue and the proposed solution. Section 5 illustrates the experimental validation results. Section 6 points out a first control approach for the LCA robot. Finally, section 7 presents some concluding remarks.

2. LCA robot presentation

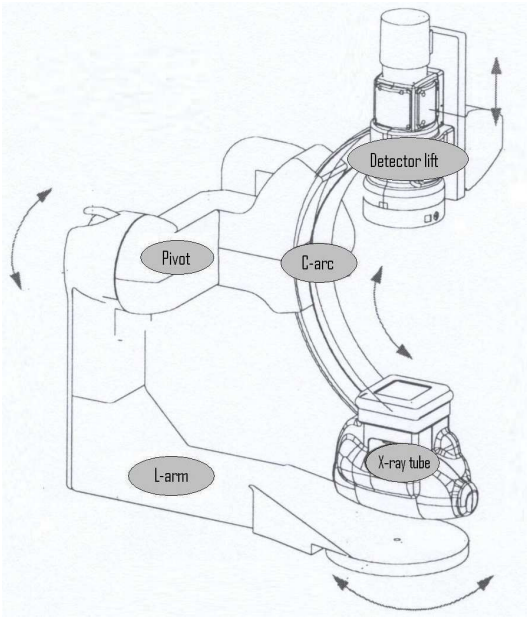

Fig. 1: LCA vascular robot

The LCA vascular robot (figure 1) is used for medical X-ray imaging. It is a four-degrees-of-freedom open-chain robot composed of the following links: L-arm: rotational joint, Pivot: rotational joint, C-arc: rotational joint and Lift:

prismatic joint. We note that the X-rays tube it fixed the C-arc. To sum up, robot has three rotational joints and one prismatic joint.

3. Modeling approach

The modeling of the LCA robot requires a clear distinction between the dynamic model of the mechanical structure and the drive chain models (figure 3). In fact, the dynamic model describes merely the relation between the applied torques and the ideal mechanical reaction of the gantry given by the joints acceleration.

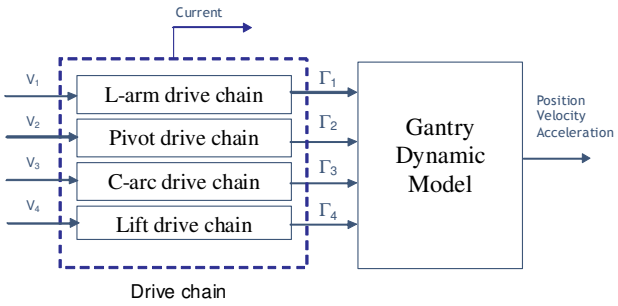

V_i are the motors command voltage. Γ_i are the axes driving torques.

Fig. 2: The robot model structure

The drive chain model takes into account the hard nonlinearities of the system such as joints friction, gear's irreversibility.

Gantry dynamic modeling

Two main methods can be used to calculate the dynamic model of the robot mechanical structure. We can mention the Newton-Euler formulation and the Lagrange formulation (Khalil, 2002).

Most authors use the Lagrange formulation that gives the mathematical expression of the model as:

$$\Gamma_{mi} = \frac{d}{dt}\left(\frac{\partial L}{\partial \dot{q}_i}\right) - \frac{\partial L}{\partial q_i} \qquad (1)$$

The latter can be reformulated into:

$$\Gamma_m = A(q)\ddot{q} + C(q,\dot{q})\dot{q} + Q(q) \qquad (2)$$

Where $q, \dot{q}, \ddot{q}$ are respectively the vectors of joints position, velocity, and acceleration.

$A(q)$: the 4x4 robot inertia matrix.

$C(q,\dot{q})\cdot\dot{q}$: the 4x1 Coriolis and centrifugal torque/ forces vector.

$Q(q)$: the 4x1 gravitational torques/ forces vector.

Γ_m : the 4x1 input torques/ forces vector.

2.2 Drive chain modeling

The next step consists of modeling the drive chain, which includes the electrical motor (DC motor for this application), the mechanical transmission (gears) and the elements of power dissipation (friction) (figure 3):

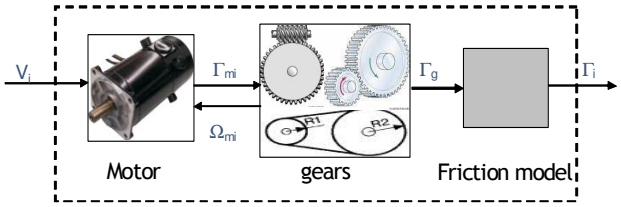

Fig. 3: Drive chain model

Electrical motors modeling is a well-known issue, hence it will not be described in this paper. We lay stress on gears and friction modeling, which are the cause of the irreversibility.

Actually, this phenomenon can be modeled using several approaches. From a microscopic point of view, it can be modeled by describing the forces of contacts among the driving and the driven elements inside the gearbox. Unfortunately, this rigorous approach leads to very complex analytical model, with serious difficulties in the implementation and simulations, particularly in the case of closed loop structures including controllers (Henriot, 1991). Besides, the identification of this type of models is very complicated due to the significant number of its parameters.

We can consider a macroscopic modeling approach where the power loss in the friction bloc (figure 3) is modeled using an efficiency coefficient taking account of the power transfer direction (load driving/driven) (Abba, 1999), (Abba, 2003). In our approach, we propose to use a state machine to define the current functional state of the transmission in order to reproduce the irreversibility. In the case of this robot, this method has been tested and the obtained model was validated experimentally.

4. The irreversibility modeling

This section is the most essential in drive chains modeling. In fact, good power dissipation modeling helps to reproduce complex gear behaviors such as irreversibility. The power dissipation will be illustrated through the friction phenomenon.

In robotics, friction is often modeled as a function of joint velocity. It is based on static (eq.3), dry and viscous friction (eq.4) (Khalil, 2002), (Armstong, 1988).

$$\Gamma_{fsi}(\Gamma_{mi},\dot{q}_{mi}) = \begin{cases} \min(\Gamma_{mi},\Gamma_{sdi}) & \text{if } \Gamma_{mi}>0, \dot{q}_{mi}=0 \\ \max(\Gamma_{mi},\Gamma_{sri}) & \text{if } \Gamma_{mi}<0, \dot{q}_{mi}=0 \\ 0 & \text{if } \dot{q}_{mi}\neq 0 \end{cases} \qquad (3)$$

where $\dot{q}_{mi}, \Gamma_{sdi}$ and Γ_{sri} are respectively the velocity, the static friction torque for the direct and the reverse motion of the joint "i" .

$$\Gamma_{fvi}(\dot{q}_{mi}) = \begin{cases} f_{cdi} + f_{vdi}\cdot\dot{q}_{mi} & \text{if } \dot{q}_{mi}>0 \\ -f_{cri} + f_{vri}\cdot\dot{q}_{mi} & \text{if } \dot{q}_{mi}<0 \\ 0 & \text{if } \dot{q}_{mi}=0 \end{cases} \qquad (4)$$

where f_{cdi} and f_{cri} are the Coulomb friction coefficients for the direct and the reverse motion of the joint "i", f_{vdi} and f_{vri} are the viscous friction coefficients for the direct and the reverse motion of the joint "i".

These models produce accurate simulation results with simple drive chain structures. However, in the presence of complex mechanisms such as worm gears these models lack

of reliability. To illustrate this phenomenon, we can compare the theoretical motor torque required to drive the LCA pivot axis in the case of a reversible transmission and the real measured motor torque which is obtained via the motor current measurement. Figure 4 and 5 show the applied torques on the pivot axis during a 7°/sec and -7°/sec constant velocity movement. During this movement, the robot dynamic is represented by the following dynamic equation:

$$\Gamma_m = \Gamma_l + \Gamma_f \tag{5}$$

where $\Gamma_l = Q(q)$ is the load torque and Γ_f is the friction torque.

Consequently, we expect that the motor torque will have the same behavior as the load torque since the friction torque does not vary at constant speeds (eq.5). However, these results reveal an important difference between the measured motor torque and the expected motor torque with a drive chain using only velocity friction model. We notice that at the position 60 degrees, the load becomes driving, which means that the direction of the power flow changes. Actually, the irreversibility compensates the gravity torque in this case. Therefore, it is essential to expand the friction model to take into consideration more variables such as motor torque and load torque in order to reproduce the irreversibility in a simulation environment.

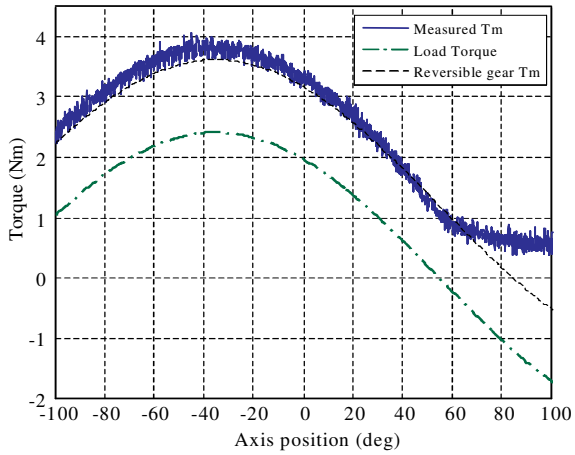

Fig. 4: Motor and load torque variation during constant velocity rotation (7 °/s)

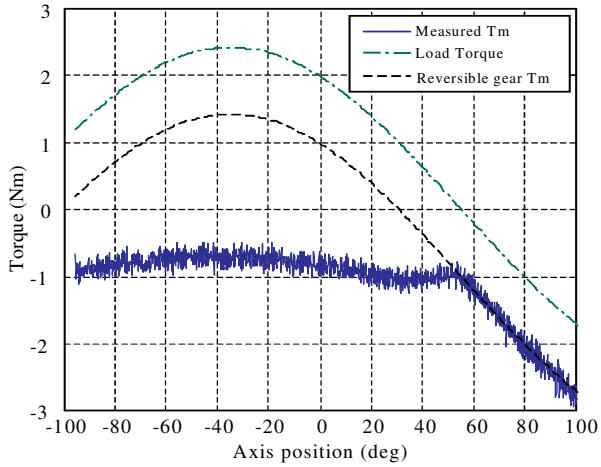

Fig. 5: Motor and load torque variation during constant velocity rotation (-7 °/s)

Consequently, the new friction model Γ_f applied on motor shaft will have the following structure:

$$\Gamma_f = \Gamma_{fs}(\Gamma_m, \dot{q}_m) + \Gamma_{fv}(\dot{q}_m) + \Gamma_{fT}(\Gamma_m, \Gamma_l, \dot{q}_m) \tag{6}$$

where :

$\Gamma_{fs}(\Gamma_m, \dot{q}_m)$: 4x1 vector of the static friction model

$\Gamma_{fv}(\dot{q}_m)$: 4x1 vector of the velocity friction model

$\Gamma_{fT}(\Gamma_m, \Gamma_l, \dot{q}_m)$: 4x1 vector of the torque friction model

Γ_{fs} and Γ_{fv} are the classical friction terms usually used in drive chain modeling (Armstong, 1988),(Dupont, 1990). Whereas, Γ_{fT} presents the term that takes account of the irreversibility behavior.

The proposed torque friction model is:

$$\begin{aligned}\Gamma_{fTi}(\Gamma_{mi}, \Gamma_{li}, \dot{q}_{mi}) = {} & \mu_{mi}(\Gamma_{mi}, \Gamma_{li}, \dot{q}_{mi}) \cdot \Gamma_{mi} \\ & + \mu_{li}(\Gamma_{mi}, \Gamma_{li}, \dot{q}_{mi}) \cdot \Gamma_{li}\end{aligned} \tag{7}$$

where $\mu_{mi}(\Gamma_{mi}, \Gamma_{li}, \dot{q}_{mi})$ and $\mu_{li}(\Gamma_{mi}, \Gamma_{li}, \dot{q}_{mi})$ are the motor and load friction dynamic coefficients.

Let's consider now the complete robot dynamic model:

$$\Gamma_m = J_m \cdot \ddot{q}_m + N^{-1} A(q) \ddot{q} + \Gamma_l + \Gamma_f \tag{8}$$

where $\Gamma_l = N^{-1}(C(q, \dot{q})\dot{q} + Q(q))$ and J_m is the 4x4 motors inertia matrix. By replacing (7) in (8) we obtain:

$$\begin{aligned}\Gamma_m = {} & (J_m + N^{-2} A(q)) \cdot \ddot{q}_m + \Gamma_l + \Gamma_{fs}(\Gamma_m, \dot{q}_m) \\ & + \Gamma_{fv}(\dot{q}_m) + \mu_m \cdot \Gamma_m + \mu_l \cdot \Gamma_l\end{aligned} \tag{9}$$

where μ_m and μ_l are respectively 4x4 diagonal matrixes:

$$\mu_m = \mathrm{diag}\{[\mu_{mi}(\Gamma_{mi}, \Gamma_{li}, \dot{q}_{mi})]\,; i = 1, \ldots, 4\}$$
$$\mu_l = \mathrm{diag}\{[\mu_{li}(\Gamma_{mi}, \Gamma_{li}, \dot{q}_{mi})]\,; i = 1, \ldots, 4\}$$

By regrouping the terms of equation 9, we obtain:

$$\begin{aligned}\eta_m \cdot \Gamma_m = {} & (J_m + N^{-2} A(q)) \cdot \ddot{q}_m + \eta_l \cdot \Gamma_l \\ & + \Gamma_{fs}(\Gamma_m, \dot{q}_m) + \Gamma_{fv}(\dot{q}_m)\end{aligned} \tag{10}$$

where $\eta_m = (I_{4\times4} - \mu_m)$ and $\eta_l = (I_{4\times4} + \mu_l)$.

The new terms η_m and η_l which depend on Γ_m, Γ_l and $\dot{q}_m$ introduce the efficiency concept in the robot dynamic model. The next section will focus on the proposed approach used to calculate the drive chain efficiency coefficients.

4.1 Efficiency coefficients estimation

One of the complex issues in drive chain modeling is the estimation of the efficiency coefficient. One technique consists in theoretically calculating the efficiency of each element of the drive chain using the efficiency definition (Henriot, 1991):

$$\eta = \frac{|\text{Received Power}|}{\text{Emitted Power}} = \frac{|P_{out}|}{P_{in}} \tag{11}$$

The calculation of this coefficient requires the determination of the driving element whether it is the motor or the load. We

talk then about the motor torque efficiency (η_m) or the load torque efficiency (η_l). Therefore, the received power "P_{in}" could be either from the motor or the load.

Actually, this method can be applied with simple gear mechanisms such as spur gears, whereas for complex gears, such as worm gears, the calculation of the efficiency coefficient using analytical formulas tends to be hard and inaccurate due to the lack of information concerning the friction modeling as well as the complexity of the contact surface between gears' components. Besides, to our knowledge, this problem was treated theoretically only in the steady state and it has rarely been treated in the transient state.

The alternative that we propose is to experimentally identify the efficiency coefficient according to a functional state of the drive chain, for instance, when the load is driving the movement or when the motor is driving the movement. This leads us to create a state machine with the following inputs and outputs:

Inputs	Outputs
Γ_m : motor torque (Tm)	η_m : motor efficiency
Γ_l : load torque (Tl)	η_l : load efficiency
$\dot{q}_m$: motor velocity	

Now, we will present the states and the criteria of states transitions that we have used for LCA robot drive chain modeling. The state machine includes two levels:

- The upper level that describes the motion (figure 6)
- The lower level describes the switch between motor driving and load driving states (figures 7, 8), and associates an efficiency coefficient for each state.

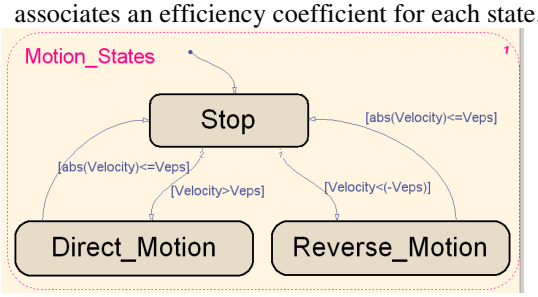

Fig. 6: Motion state machine

In the upper level, the transition condition is the sign of the velocity. In fact, for simulation convergence issue the drive chain is considered stopped when $|\dot{q}_m| < V_{eps}$, where V_{eps} is the stop velocity threshold.

For each motion state, we build the movement driving sub-states.

1) The stop state (figure 7):

During the stop phase, the drive chain is irreversible (the load torque cannot drive the movement). Motion is observed when the motor torque becomes superior to the load torque.

In the lower level, the state transition is based on the motor and load torque values. As for V_{eps} (figure 7), Tm_{eps} represents the motor torque threshold, it is used for simulation convergence issues ($Tm_{eps} = 10^{-5}$ Nm).

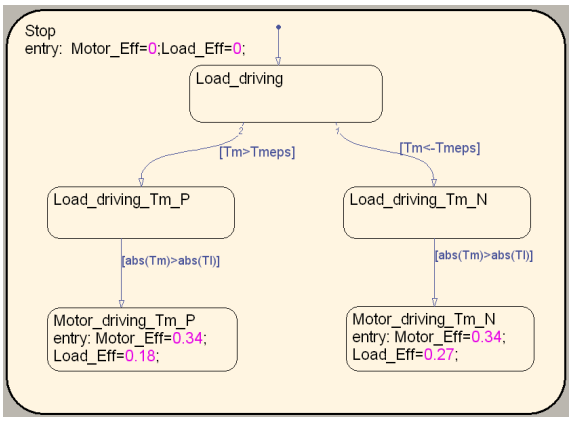

Fig. 7: Stop state machine

2) The direct motion state:

For direct motion state (if V>0), we have four main states (figure 8), the states transitions are given by the following conditions:

- $\Gamma_m > 0$ and $\Gamma_l < 0$: the motor is driving
- $\Gamma_m > 0$ and $\Gamma_l > 0$: we distinguish 2 states whether $\Gamma_l > \Gamma_m$ or not.
- $\Gamma_m < 0$: the motor is braking (load driving)

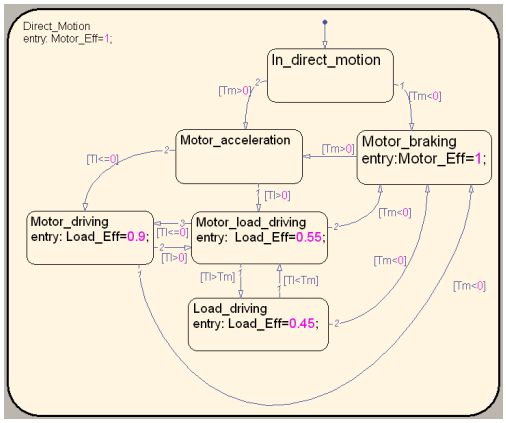

Fig. 8: direct motion state machine

3) The reverse motion state:

The reverse motion (V<0) state machine has the same structure as the direct motion one. We need to replace Γ_m and Γ_l by $-\Gamma_m$ and $-\Gamma_l$. The table 1 summaries the drive chain efficiency coefficients for each state:

1. Motor driving
2. Motor and load driving
3. Load driving

States	Direct motion η_l	Reverse motion η_l
1- $\Gamma_m \cdot \Gamma_l < 0$	0.9	0.9
2- $\Gamma_m \cdot \Gamma_l > 0$ & $\|\Gamma_m\| < \|\Gamma_l\|$	0.55	0.16
3- $\Gamma_m \cdot \Gamma_l > 0$ & $\|\Gamma_m\| > \|\Gamma_l\|$	0.45	0.06

Table 1: Drive chain efficiency coefficients

5. Experimental validation

The validation of the drive chain model has been done on the pivot axis. Indeed, it allows the system to have different states transition (load driving/driven) during the same movement. The efficiency coefficients have been identified using experimental measures.

We compare the open loop response of the pivot joint and the simulation results to a voltage input for both direct and reverse motion. Figure 9 shows the applied voltage on the pivot motor for a direct motion test. Figure 10 shows the experimental results (dashed curve) of the current, the velocity and the position and those obtained in simulation (solid curve). We notice in that the simulation response represents the same behavior as the real mechanism. In this figure we distinguish four main phases:

- The starting phase 24s to 25s
- The motor driving phase 25s to 37.8s
- The load driving phase 37.8s to 4.2s
- The braking phase 40.2s to 40.3s

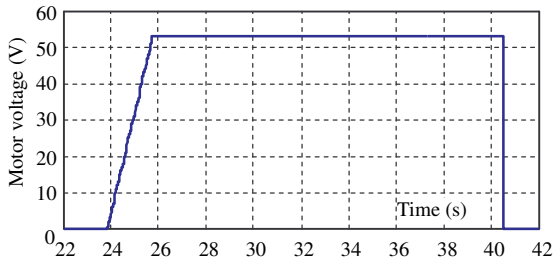

Fig.9: Open loop motor command voltage

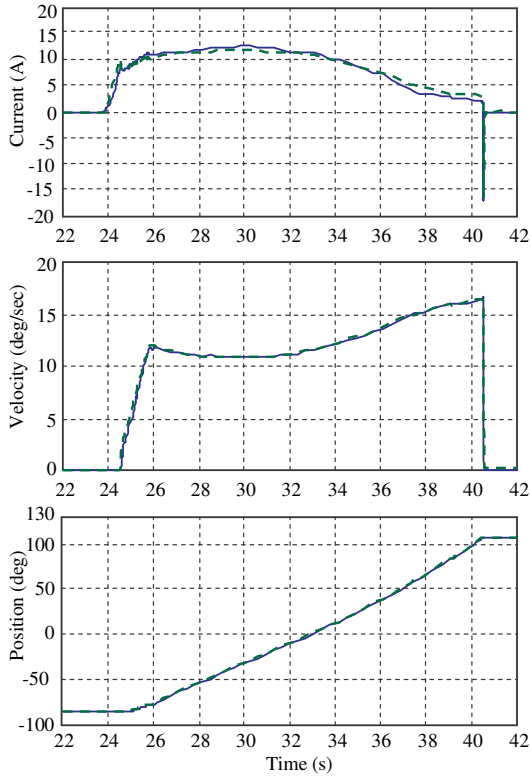

Fig. 10: Direct motion outputs

6. Control approach

In this section, we will present a first control law based on two cascaded loops. An internal current loop associated to an external speed loop. Each one comprises a proportional integral "PI" regulator (figure 11) (Poignet, 2002)0. This approach will be implemented and tested using the pivot axis simulator presented in the previous sections.

The transfer function of the PI controller is (Ogata, 1997) $G = K_p \cdot [1 + 1/(T_i \cdot s)]$ where K_p represents the proportional gain and T_i represents the integral action time.

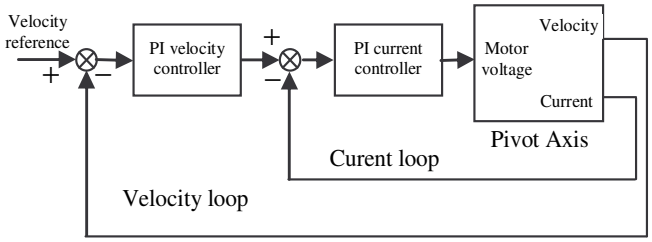

Figure 11: Cascaded loops controller

6.1 Current loop regulator

The first step consists of calculating the current loop parameters. We extract the linear models of the pivot around different operating points. Figure 12 shows the open loop Bode diagrams of the current loop around the different operating points. These diagrams illustrate that at high frequency, the frequency responses are independent from the operating point. Consequently, we can calculate the controller parameter regardless of the pivot position. Since the response time to torque disturbances is directly related to the integration time constant T_i, the approximation $t_r \approx 3T_i$ can then be used, where $t_r = 3ms$. Then, K_{p_i} is estimated so as to ensure the cut-off frequency at $\omega_c = 1/T_{i\_i} = 1000\,\text{rad}\cdot\text{s}^{-1}$, Graphically, we obtain $K_{p\_i} = 30\,dB = 31.62$

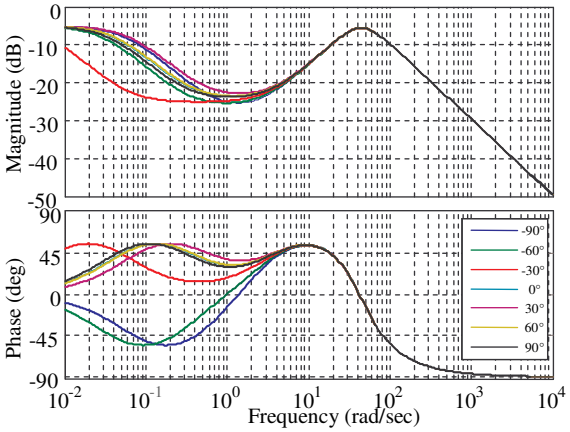

Fig. 12: Current open loop bode responses for linearized pivot model

Figure 17, shows the simulated current response to a step reference of 5 A. We notice a response time $t_r \approx 3\,\text{ms}$ and an over shoot $D = 24\,\%$

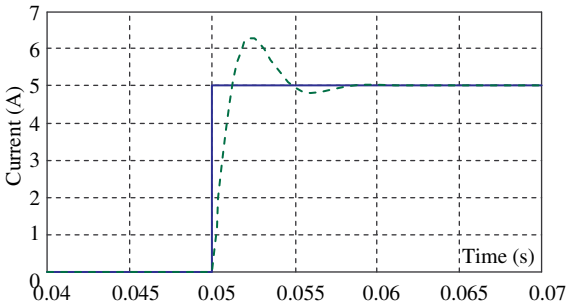

Fig. 13: Current step response

6.2 *Velocity loop regulator*

The same approach is used to calculate the PI velocity controller parameters. As for the current controller, we notice (figure 14) that the velocity controller can be calculated regardless of the operating points for frequencies higher than 20 rad/sec. Hence, we choose: $\omega_c = 1/T_{i\_v} = 100\,\text{rad}\cdot\text{s}^{-1}$ and graphically (figure 14), we deduce $K_{p\_i} = 50\,\text{dB} = 316.23$.

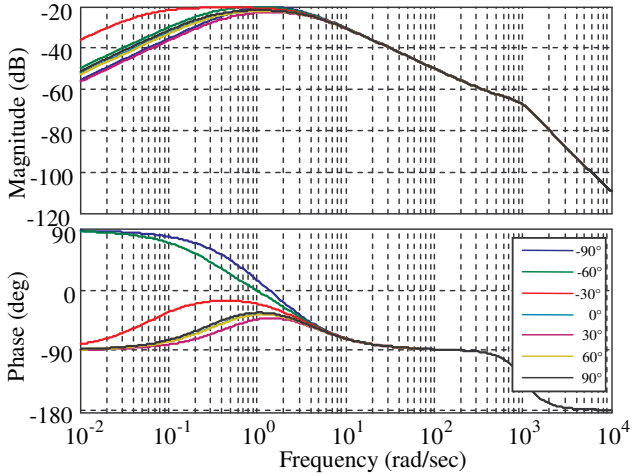

Fig. 14: Velocity open loop bode responses for linearized pivot model

Figure 15 illustrates the simulated current, velocity and position responses to a ramp velocity input. The total displacement is about 25 degrees, the range was chosen so as to observe the state switching "motor driving to load driving". The transition occurs at 55 degrees corresponding to the vertical position (90 degrees) of the center of gravity.

7. Conclusions

In this paper, we presented a methodology in order to model the irreversibility property in mechanical drive chains. The proposed approach uses a macroscopic modeling of the gears, which are usually the origin of irreversibility in a drive chain. It consists in creating a state machine representing different functional states of the gears and attributing an efficiency coefficient to each specific state.

The validation of the proposed modeling was carried out on the Pivot axis of the LCA robot. The methodology has been tested when the position trajectory leads to some transitions "motor driving to load driving" and the obtained results prove the accuracy of the model.

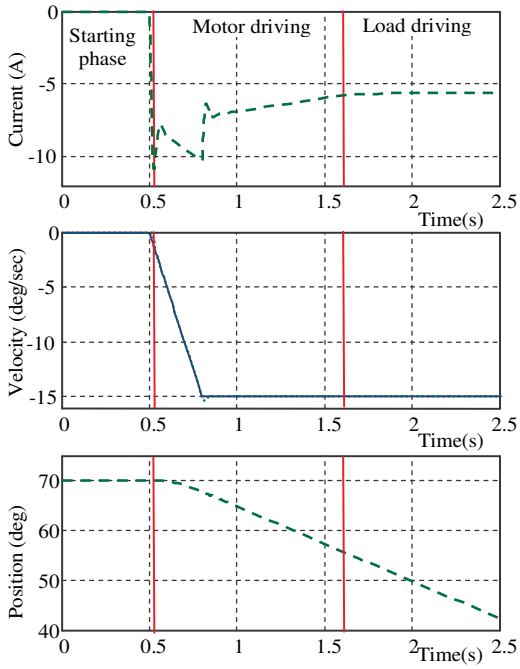

Fig. 15: Velocity ramp response

Besides, a first control approach based on PI controllers was presented. The controller parameters were calculated using a classical frequency response method using a set of models around different operating points.

The perspectives of this work concern two research orientations. The first one is the definition and the study of an automatic procedure to identify the efficiency coefficient for each state. The second one is the investigation of the trajectory planning and the control of robots with irreversible transmissions when considering state machines for gear's modeling.

REFERENCES

Abba, G., Chaillet, N. (1999). Robot dynamic modeling using using a power flow approach with application to biped locomotion", *Autonomous Robots* 6, pp. 39–52.

Abba, G., Sardain, P., (2003). Modélisation des frottements dans les éléments de transmission d'un axe de robot en vue de son identification: Friction modelling of a robot transmission chain with identification in mind, *Mécanique & Industries*, **Volume 4**, Issue 4, pp 391-396

Armstrong, B. (1988). Friction: Experimental determination, modelling and compensation, *IEEE International Conference on Robotics and Automation*, Philadelphia, PA, USA, **Volume 3**, pp. 1422–1427.

Dupont, P.E. (1990). Friction modeling in dynamic robot simulation, *Robotics and Automation*,. Proceedings., IEEE International Conference, **Volume 2**, pp. 1370-1376

Henriot, G.,(1991). *Traité théorique et pratique des engrenages*, 5th ed. Dunod ed. vol. 1.

Khalil, W., Dombre, E., (2002). *Modeling, identification and control of robots*, *Taylor & Francis Group* ed.

Ogata, K. (1997) *Modern control Engineering*, 3rd ed. Prentice-Hall Inter. ed.

Poignet, Ph., Gautier, M., Khalil, W., Pham, M.T. (2002). Modeling, simulation and control of high speed machine tools using robotics formalism", *Mechatronics*, pp 461–487